JOURNAL OF VIROLOGY, June 1999, p. 4728–4737 Vol. 73, No. 6
0022-538X/99/$04.00+0

Reversion of a Human Immunodeficiency Virus Type 1 Matrix Mutation Affecting Gag Membrane Binding, Endogenous Reverse Transcriptase Activity, and Virus Infectivity

ROSEMARY E. KIERNAN,† AKIRA ONO, AND ERIC O. FREED*

Laboratory of Molecular Microbiology, National Institute of Allergy and Infectious Diseases, National Institutes of Health, Bethesda, Maryland 20892-0460

Received 29 December 1998/Accepted 12 March 1999

We previously characterized mutations in the human immunodeficiency virus type 1 matrix (MA) protein that displayed reduced infectivity in single-round assays, defects in the stable synthesis of viral DNA in infected cells, and impaired endogenous reverse transcriptase activity. The mutants, which contained substitutions in a highly conserved Leu at MA amino acid 20, also increased binding of Gag to membrane. To elucidate further the role of MA in the virus replication cycle, we have characterized a viral revertant of an amino acid 20 mutant (20LK). The revertant virus, which replicates with essentially wild-type kinetics in H9 cells, contains second-site compensatory changes at MA amino acids 73 (E→K) and 82 (A→T), while retaining the original 20LK mutation. Single-cycle infectivity assays, performed with luciferase-expressing viruses, show that the 20LK/73EK/82AT triple mutant displays markedly improved infectivity relative to the original 20LK mutant. The stable synthesis of viral DNA in infected cells is also significantly increased compared with that of 20LK DNA. Furthermore, activity of revertant virions in endogenous reverse transcriptase assays is restored to near-wild-type-levels. Interestingly, although 20LK/73EK/82AT reverses the defects in replication kinetics, postentry events, and endogenous reverse transcriptase activity induced by the 20LK mutation, the reversion does not affect the 20LK-imposed increase in Gag membrane binding. Mutants containing single and double amino acid substitutions were constructed, and their growth kinetics were examined. Only virus containing all three changes (20LK/73EK/82AT) grew with significantly accelerated kinetics; 73EK, 73EK/82AT, and 20LK/82AT mutants displayed pronounced defects in virus particle production. Viral core-like complexes were isolated by sucrose density gradient centrifugation of detergent-treated virions. Intriguingly, the protein composition of wild-type and mutant detergent-resistant complexes differed markedly. In wild-type and 20LK complexes, MA was removed following detergent solubilization of the viral membrane. In contrast, in revertant preparations, the majority of MA cosedimented with the detergent-resistant complex. These results suggest that the 20LK/73EK/82AT mutations induced a significant alteration in MA-MA or MA-core interactions.

The matrix (MA) domain of the human immunodeficiency virus type 1 (HIV-1) Gag protein is initially synthesized as part of a precursor molecule, $Pr55^{Gag}$, which is cleaved by the viral protease (PR) to generate the mature Gag proteins p17 (MA), p24 capsid (CA), p7 nucleocapsid (NC), and p6. MA is localized in the virion to the inner face of the viral envelope, where it associates with the lipid bilayer by a multipartite membrane-binding domain (for a review, see reference 12).

Although under some circumstances, both early and late aspects of the HIV-1 life cycle can be achieved with HIV-1 Gag mutants lacking much or all of MA (32, 42, 48), the HIV-1 MA protein clearly performs several important roles in virus replication. MA is necessary for specific targeting of the Gag precursor to the plasma membrane (3, 12, 18, 22) and is required for efficient incorporation of the HIV-1 envelope (Env) glycoprotein into virions (9, 14, 16, 52). Several reports have also implicated HIV-1 MA in an early step in the virus life cycle prior to the completion of reverse transcription. Initially, it was demonstrated that a deletion near the C terminus of HIV-1 MA delayed virus replication and reduced viral DNA synthesis in infected cells (51). Several linker insertion mutations in MA impaired HIV-1 infectivity; in this study, the infectivity defect correlated with altered virion morphology (41). More recently, single and double amino acid substitutions near the N terminus of MA were reported to reduce infectivity in single-round assays and interfere with the synthesis of viral DNA postinfection (6). Mutations elsewhere in HIV-1 Gag, for example, in CA and NC, have also been observed to block early steps in virus replication (12). The mechanism by which these diverse mutations interfere with an early postentry event(s) has not been elucidated. It is noteworthy that in many cases, HIV-1 Gag mutants which exhibit postentry defects display pleiotropic phenotypes in which aspects of virus assembly and/or virion maturation are also affected (for a review, see reference 12).

We previously characterized (30) a series of mutants containing single amino acid substitutions in the highly conserved Leu at HIV-1 MA residue 20. These residue 20 mutants showed delayed replication kinetics in a range of cell types, and impaired infectivity in single-cycle assays. PCR analysis of reverse-transcribed DNA in infected cells revealed reduced levels of viral DNA, particularly at 24 to 48 h postinfection. This latter result raised the possibility that the complex in which reverse transcription takes place was unstable over time. The residue 20 mutants also displayed defects in endogenous reverse transcriptase (ERT) assays, which measure reverse transcription in detergent-permeabilized virions by using the viral RNA genome as a template. Interestingly, the degree to which ERT activity was reduced correlated directly with the severity of the infectivity defect. The mutations at MA residue 20 also

* Corresponding author. Mailing address: Bldg. 4, Rm. 307, NIAID, NIH, Bethesda, MD 20892-0460. Phone: (301) 402-3215. Fax: (301) 402-0226. E-mail: EFreed@nih.gov.

† Present address: IGH, CNRS-UPR 1142, Montpellier, France.

caused accelerated Gag precursor processing and an apparent increase in Gag-to-membrane binding in virus-expressing cells (30).

Viral revertants provide a powerful tool for the identification of second-site changes which compensate for defects imposed by mutation. Information obtained in the analysis of revertants sheds light on the relationship between protein structure and function and defines potential inter- and intramolecular interactions. We previously identified and characterized second-site compensatory changes in HIV-1 MA which reversed defects in Env incorporation (14, 39) and virus assembly (39) resulting from single amino acid substitutions in MA. To gain additional insights into the role MA plays in the virus life cycle, we have obtained and characterized a viral revertant of a residue 20 mutant (20LK). This revertant, which acquired second-site changes at MA residues 73 and 82, reverses the infectivity and ERT defects induced by the 20LK mutation but does not repair the increased Gag processing and membrane binding properties of 20LK. Data obtained by treatment of virions with detergent, followed by sucrose gradient ultracentrifugation, are consistent with the speculation that the 20LK/73EK/82AT revertant alters MA-MA or MA-core interactions.

MATERIALS AND METHODS

Molecular cloning of a 20LK revertant and site-directed mutagenesis. Molecular cloning of the 20LK revertant was performed as described previously (14). Briefly, virus supernatant was harvested at the peak of RT activity from H9 cultures infected with the 20LK mutant. Virus stocks were normalized for RT activity and used to infect fresh H9 cells in parallel with the wild-type (wt) virus. Near the peak of RT activity in the infected culture, Hirt DNA (25) was purified and a 1.2-kbp fragment spanning the MA coding region was amplified by PCR. The amplified DNA was cloned into pUC19 and sequenced. After sequencing, *Bss*HII-*Sph*I fragments from the pUC19 clones were exchanged for the *Bss*HII-*Sph*I fragment of pNL4-3 (1) to generate molecular clones containing the revertant-derived changes. HIV-1 MA mutations were introduced into pNL4-3, *env*-minus clones of pNL4-3 (pNL4-3KFS) (13), or luciferase-expressing *env*-minus clones of pNL4-3 (pNLuc) (30) as described previously (30). Amino acid mutations at MA residues 73 (73EK) and 82 (82AT) and the 20LK/73EK, 20LK/82AT, and 73EK/82AT double amino acid substitutions, were introduced into pNL4-3 by site-directed mutagenesis as described previously (18). The 20LK/73EK/82AT triple mutant was constructed by cloning the *Bss*HII-*Sph*I fragment from a pUC19 clone containing these changes into pNL4-3.

The construction of pNL4-3 derivatives containing stop codons after MA (pNL4-3/MAstop) or after CA (pNL4-3/p41stop) has been described in detail elsewhere (38). Briefly, pNL4-3/MAstop was constructed by introducing stop codons at CA amino acid positions 1 and 2 by the same strategy used for MA mutagenesis (18). Introduction of 20LK and 20LK/73EK/82AT changes into pNL4-3/MAstop was performed by using a 1.6-kbp *Stu*I-*Sph*I fragment of pNL4-3/MAstop subcloned into M13mp19 as a template for mutagenesis. To construct the plasmid pNL4-3/p41stop (38), which expresses only MA and CA [p41 (MA-CA)], a stop codon was introduced at residue 1 of the p2 spacer peptide. Oligonucleotide-directed mutagenesis was performed by using an M13mp18 subclone harboring the *Sph*I-*Pst*I (1.4-kbp) fragment from pNL4-3 as a template. After mutagenesis, the M13pm18-derived *Sph*I-*Pst*I fragment containing the stop codon was introduced into pNL4-3 and sequenced in its entirety. The same fragment was cloned into pNL4-3/20LK and pNL4-3/20LK/73EK/82AT to generate p41stop versions of these MA mutants.

Transfections and infections. HeLa and H9 cells were maintained as described previously (15, 30). 293T cells were cultured in Dulbecco modified Eagle medium containing a high concentration of glucose, L-glutamine, 25 mM HEPES, and pyridoxine hydrochloride (Gibco BRL catalog no. 12430-054) supplemented with 10% fetal bovine serum. Virus stocks of pNL4-3 or derivatives containing mutations in MA were obtained following transfection of HeLa cells as described previously (15). Pseudotyped virus stocks of pNL4-3KFS, pNLuc, and mutant MA derivatives were prepared by cotransfection of HeLa cells or 293T cells with a vector expressing HIV-1 Env (pHenv [17] or pIIIenv3-1, a gift of J. Sodroski [46]) as described previously (30). Infections of H9 cells were performed as described previously (30). RT assays were performed as reported previously (15).

Single-cycle luciferase infectivity assays. pNLuc molecular clones (30) containing either wt or mutant MA coding regions were cotransfected into 293T cells with the HIV-1 Env expression vector pHenv (17) or pIIIenv3-1 (46). Virus stocks were harvested, normalized for RT assay, and used to infect H9 cells. Relative infectivity was measured by luciferase assay as described previously (30).

Immunoprecipitations. Methods used for metabolic labeling of transfected HeLa cells, preparation of cell and virion lysates, and immunoprecipitation of viral proteins with AIDS patient sera (obtained from the National Institutes of Health AIDS Research and Reference Reagent Program) have been described previously (15, 49).

PCR analysis and ERT assays. For PCR analysis, HeLa cells were cotransfected with the HIV-1 Env expression vector pIIIenv3-1 (46) and the *env*-minus HIV-1 molecular clone pNL4-3KFS (13, 16) containing wt or mutant MA coding regions. Pseudotyped virions, normalized for RT activity, were used to infect H9 cells. At several time points postinfection, cells were lysed and analyzed by PCR using primers specific for the HIV-1 long terminal repeat (30) or α-tubulin DNA (Clontech). PCR and Southern blotting were performed as described previously (30). For detection of α-tubulin DNA, the PCR product amplified from the positive control provided (Clontech) was ^{32}P labeled by random priming and used as a probe.

ERT assays were performed as described previously (30). Briefly, virus was normalized based on exogenous RT activity or p24 concentration, pelleted in a microcentrifuge, and permeabilized for 10 min at room temperature with the indicated detergent, and then an ERT reaction mixture containing a final concentration of 50 mM Tris-HCl (pH 8.0); 2 mM magnesium acetate; 10 mM dithiothreitol; 0.1 mM each dCTP, dGTP, and dATP; and 10 μCi [^{32}P]TTP in a final volume of 100 μl was added. After 16 h of incubation at 37°C, samples were treated with RNase A and then digested with proteinase K. Reaction products were purified by using a Wizard PCR Prep DNA Purification kit (Promega) and denatured in 0.1 M NaOH prior to agarose gel electrophoresis. The gels were dried and exposed to film.

Preparation of viral core-like structures and sucrose density gradient analysis. 293T cells were transfected with pNL4-3 or mutant MA derivatives. At 24 h posttransfection, the cells were radiolabeled with 750 μCi of [^{35}S]Cys for 24 h at 37°C. Radiolabeled transfection supernatant was filtered through 0.45-μm-pore-size filters and pelleted at 100,000 × *g* for 45 min. Virions were resuspended in phosphate-buffered saline and incubated with an equal volume of 0.15% Nonidet P-40 (NP-40; final concentration, 0.075%) for 15 min at room temperature before being loaded onto linear 20-to-70% (wt/wt) sucrose gradients. Similar results were obtained with 0.5 or 1% Triton X-100 or 0.125% Brij 97 (data not shown). Gradients were centrifuged at 100,000 × *g* for 16 h at 4°C. Twelve fractions were collected from the top of each tube, and the pellet was solubilized in sample buffer. 20LK/73EK/82AT MA protein is less efficiently recognized by anti-Gag antibody (29). Therefore, to avoid problems of differential antibody reactivity, samples were analyzed directly by sodium dodecyl sulfate-polyacrylamide gel electrophoresis (SDS-PAGE) and fluorography. Fractions were assayed for RT activity as described above. The density of each fraction was determined with a refractometer.

Membrane binding analysis. Our methods for equilibrium flotation centrifugation, which were a modification of those reported by Spearman et al. (47), have been described in more detail elsewhere (38). Briefly, transfected HeLa cells were scraped and resuspended in 10 mM Tris-HCl containing 1 mM EDTA, 10% (wt/vol) sucrose, and Complete protease inhibitor cocktail (Boehringer Mannheim). Postnuclear supernatants were obtained after sonication of cell suspensions. Postnuclear supernatant (250 μl) was mixed with 1.25 ml of 85.5% (wt/vol) sucrose in Tris-EDTA (TE) and placed on the bottom of a centrifuge tube. On top of this postnuclear supernatant-containing 73% (wt/vol) sucrose mixture was layered 7 ml of 65% (wt/vol) sucrose in TE and 3.25 ml of 6% (wt/vol) sucrose in TE. The gradients were centrifuged at 100,000 × *g* for 18 h at 4°C in a Beckman SW41 rotor. Ten 1.2-ml fractions were collected from the top of the centrifuge tube for Western blotting or radioimmunoprecipitation as described above. To verify that all of the Gag protein subjected to the flotation analysis was recovered in the 10 gradient fractions, postnuclear supernatants were also spun in an ultracentrifuge and the total amount of pelleted and supernatant Gag was determined (38). Gels were scanned with a densitometer, and sucrose densities were measured with a refractometer.

RESULTS

Isolation of a 20LK revertant. Previous studies demonstrated that the 20LK HIV-1 MA mutation causes a significant delay in peak RT activity compared with that of the wt (30). To assess whether the virus replication detected at this delayed time point was due to the emergence of a viral revertant, supernatant was harvested at the peak of virus replication, normalized to the wt for RT activity, and used to reinfect fresh H9 cells. The repassaged, mutant-derived virus grew with near-wt replication kinetics (data not shown), suggesting the presence of revertant virus in the infected cultures.

To examine the possibility that the putative revertant harbored a second-site compensatory mutation(s), Hirt supernatant DNAs were prepared from the infected cultures near the peak of RT production and PCR was performed to amplify the

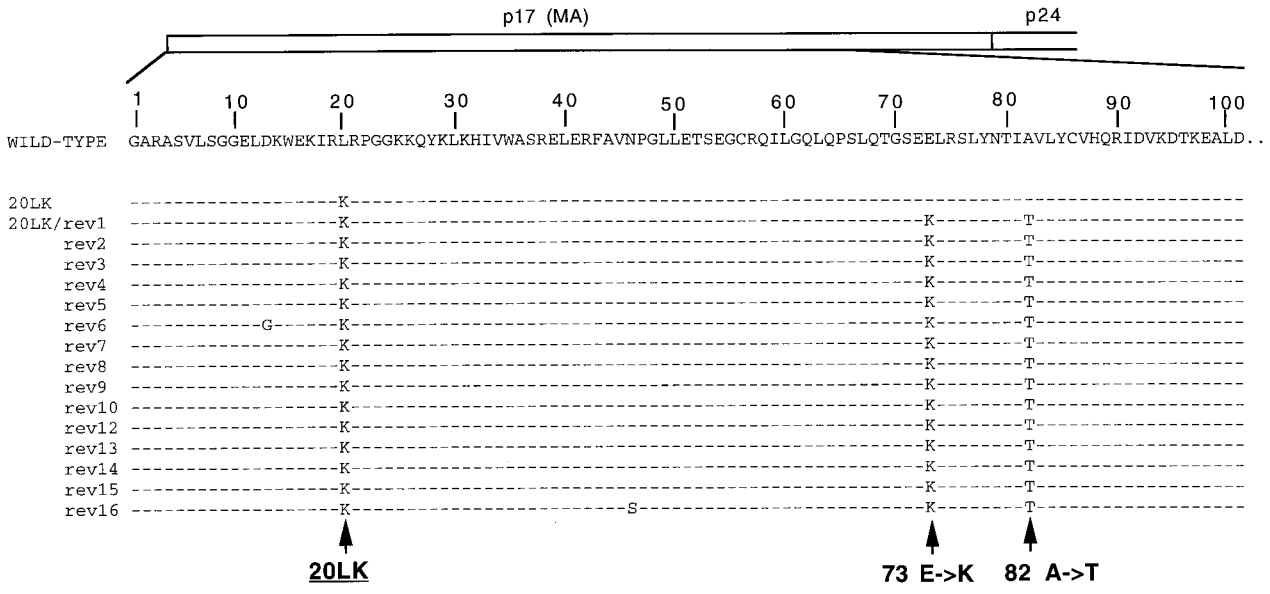

FIG. 1. Sequence analysis of 20LK revertant-derived clones. The bar represents the p17 (MA) protein. Below the bar is the amino acid sequence of wt pNL4-3 MA (amino acids 1 through 100). Below that sequence is the sequence of the original mutant and the sequences of the revertant-derived clones. A dash indicates amino acid identity with wt pNL4-3 (37); changes relative to wt are indicated in the single-letter amino acid code.

MA coding region. The amplified DNA was then cloned into pUC19, and 16 clones were sequenced. Fifteen of the 16 clones contained second-site changes at residues 73 (E→K) and 82 (A→T) while retaining the original 20LK mutation (Fig. 1). One clone contained a primary site reversion (Lys→Leu) at residue 20 (data not shown). The predominance of the 73EK and 82AT mutations in the revertant-derived clones suggests that the increased virus replication kinetics observed with the repassaged, 20LK-derived virus stock resulted from an early reversion event caused by these two changes.

The 20LK replication defect is repaired by the 73EK/82AT changes. To evaluate whether the residue 73 and 82 changes were responsible for the improved replication kinetics observed upon repassage of 20LK-derived virus, a 20LK/73EK/82AT triple mutant was constructed as described in Materials and Methods. H9 cells were infected in parallel with either the wt pNL4-3-derived virus, the original 20LK mutant, or the 20LK/73EK/82AT triple mutant (Fig. 2). In the NL4-3-infected culture, virus replication peaked on day 8 postinfection; peak virus production in the 20LK-infected culture occurred 8 days later. In contrast, the replication kinetics of the 20LK/73EK/82AT mutant were similar to those of the wt, indicating that the 73EK/82AT changes were sufficient to reverse the replication defect imposed by 20LK in H9 cells. We also compared the wt, 20LK, and 20LK/73EK/82AT replication kinetics in other T-cell lines and in primary human peripheral blood mononuclear cells. In Jurkat, MT-4, and peripheral blood mononuclear cells, the 20LK/73EK/82AT mutant showed significantly accelerated replication kinetics relative to 20LK (data not shown). Interestingly, however, in A3.01 and in the A3.01 subclone 12D-7 (11), both 20LK and 20LK/73EK/82AT replicated with similar kinetics, which were delayed 6 to 8 days relative to those of the wt (data not shown). It is noteworthy that the 20LK mutation caused a clear delay (6 days) in replication kinetics relative to the wt in MT-4 cells, despite the observation that MA-deleted mutants were able to replicate in MT-4 cells (42).

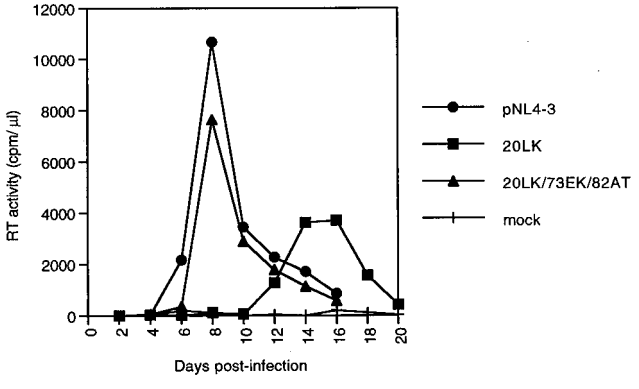

FIG. 2. Replication kinetics of the wt, 20LK, and 20LK/73EK/82AT viruses. H9 cells were infected in parallel with HeLa cell-derived wt, 20LK, and 20LK/73EK/82AT viruses. Cells were split 1:3 every 2 days; the RT activities in culture supernatants were determined for each time point.

The 20LK defect early in the virus replication cycle is reversed by the 73EK/82AT changes. We previously reported that mutation at residue 20 causes defects in the early phases of the virus life cycle (30). We sought to determine whether the 20LK/73EK/82AT revertant had repaired these defects imposed by the 20LK mutation. Single-cycle infectivity assays were performed by using HIV-1 molecular clones modified to express luciferase following infection. The pNLuc molecular clones (30) expressing either wt, 20LK, or 20LK/73EK/82AT MA were cotransfected with an HIV-1 Env expression vector. H9 cells infected with the resulting virus stocks were assayed for luciferase activity. The results of these experiments indicated that infectivity of the 20LK/73EK/82AT mutant was significantly improved in a single round of infection compared with that of 20LK (Fig. 3).

We next determined whether the improved infectivity of the 20LK/73EK/82AT revertant observed in single-cycle assays (Fig. 3) was due to an increase in the stable synthesis of viral DNA in cells infected with 20LK/73EK/82AT compared with

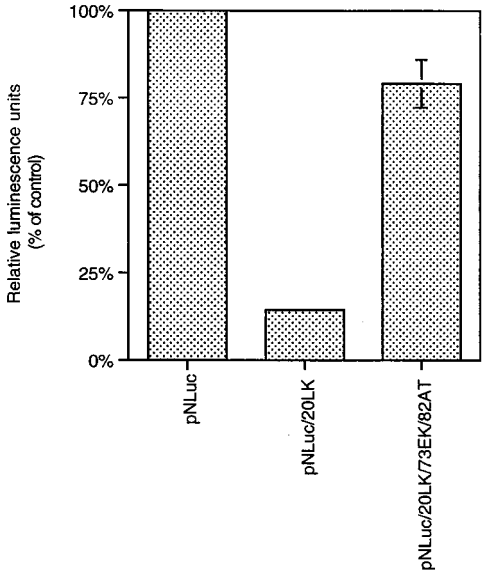

FIG. 3. Relative infectivities of the wt, 20LK, and 20LK/73EK/82AT viruses in H9 cells. Virus stocks, obtained by cotransfecting 293T cells with luciferase-expressing molecular clones (pNLuc, pNLuc/20LK, and pNLuc/20LK/73EK/82AT) and an HIV-1 Env expression vector, were normalized for RT activity and used for infection of cells as indicated in Materials and Methods. Luciferase activity obtained in infections with a nonpseudotyped pNLuc-derived virus was less than 0.5% of that obtained with a pseudotyped pNLuc-derived virus.

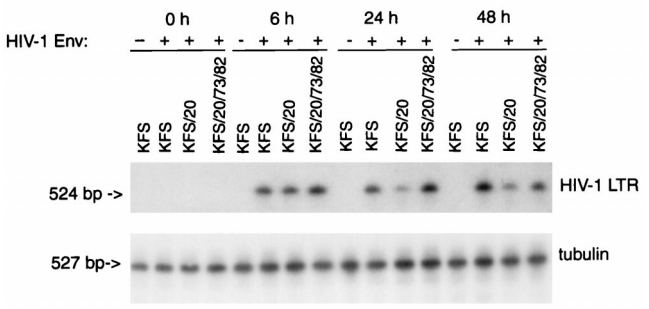

FIG. 4. PCR amplification of viral DNA postinfection. 293T cells were co-transfected with pNL4-3-derived *env*-minus molecular clones encoding wt MA (KFS) or mutant MA (KFS/20 and KFS/20/73/82) and an HIV-1 Env expression vector. Virus stocks were harvested, normalized for RT activity, and used to infect H9 cells. Nonpseudotyped KFS virions served as a negative control (leftmost lane of each set). At the indicated times postinfection, cells were lysed and viral DNA was PCR amplified by using HIV-1 LTR-specific primers (30). The amplified DNA was electrophoresed on agarose gels and subjected to Southern blotting using an HIV-1-specific probe. As a positive control for the PCRs, α-tubulin from the same set of lysates was amplified and subjected to Southern blotting. The sizes of the PCR products are shown on the left. LTR, long terminal repeat.

that in cells infected with 20LK. To ensure that all infections were exclusively single cycle, we performed the assays by using pseudotyped virions which are incapable of initiating a second round of infection. pNL4-3KFS, pNL4-3KFS/20LK, or pNL4-3KFS/20LK/73EK/82AT molecular clones, which lack the ability to synthesize any Env glycoproteins due to a frameshift mutation in the *env* gene (13, 16; Materials and Methods), were cotransfected with an HIV-1 Env expression vector. The resulting virus was then harvested, normalized for RT activity, and used to infect H9 cells. Nonpseudotyped pNL4-3KFS-derived virus was used as a negative control. At the indicated time points postinfection, the cells were lysed and viral DNA was PCR amplified by using primers specific for HIV-1 long terminal repeat sequences or, as a PCR control, cellular α-tubulin sequences. Amplified products were then electrophoresed on agarose gels and Southern blotted with specific probes (Fig. 4). Consistent with previous results (30), we observed that the amount of viral DNA detected in 20LK-infected cultures was initially (6 h postinfection) similar to that in wt-infected cells but that over time (24 to 48 h), the amount of 20LK-specific DNA was reduced. In contrast, essentially wt levels of viral DNA were present at all time points in the 20LK/73EK/82AT-infected cultures. Again, we emphasize that no virus spread could occur in this assay, since pseudotypes of *env*-minus molecular clones were used. The results presented in Fig. 3 and 4 indicate that the 20LK/73EK/82AT revertant had reversed the defects in single-cycle infectivity and in the stable synthesis of viral DNA imposed by the 20LK mutation.

The 20LK ERT defect is partially repaired by the 73EK/82AT changes. Mutation at residue 20 was previously shown to reduce activity in ERT assays. Interestingly, the severity of the ERT defect paralleled the hierarchy of biological phenotypes observed for the three residue 20 mutants tested: 20LK imposed the greatest defect in spreading viral infections and the most severe reduction in ERT assays; 20LE was the least affected biologically and showed only modestly reduced ERT activity (30). These observations established a correlation between the ERT assay phenotype and the biological defect imposed by mutations at residue 20. To determine whether this correlation would extend to the 20LK/73EK/82AT revertant, this mutant was analyzed in ERT assays. As negative controls, we also analyzed the RT active-site mutant RT/D186N (Fig. 5A) (10) and performed reactions in the presence of zidovudine triphosphate (Fig. 5B). Consistent with previous results (30), 20LK ERT activity was diminished under all of the conditions examined, i.e., when virions were permeabilized with a range of concentrations of β-octyl glucoside (Fig. 5A) or with different detergents (Fig. 5B). In contrast, 20LK/73EK/82AT displayed markedly improved ERT activity under the same conditions (Fig. 5A and B). Thus, the revertant virus largely repaired the ERT defect imposed by the 20LK mutation.

The 73EK/82AT changes do not reverse the 20LK-imposed increase in Gag processing and membrane binding. We previously demonstrated that mutation at residue 20 increases the rate of Gag processing and the kinetics of virus release (30). To examine whether this 20LK-imposed increase in the kinetics of Gag processing had been reversed by the 73EK/82AT changes, we performed pulse-chase analysis of HeLa cells transfected with wt pNL4-3 or derivatives containing the 20LK or 20LK/73EK/82AT mutations. We analyzed both the rate of Gag processing in cell-associated material and the kinetics of virion release into the extracellular medium. Both the 20LK and 20LK/73EK/82AT mutants displayed similarly increased Gag processing kinetics relative to those of the wt (data not shown).

We previously reported that the residue 20 mutations increased the relative amount of $Pr55^{Gag}$ cofractionating with membrane in cell fractionation and sucrose gradient assays (30). These results suggested that the residue 20 mutations increased Gag membrane binding, a conclusion that was confirmed by membrane flotation centrifugation (38). To determine whether the 20LK-imposed increase in Gag membrane binding was reversed with the 20LK/73EK/82AT revertant, we performed membrane flotation centrifugation analyses of wt, 20LK, and 20LK/73EK/82AT $Pr55^{Gag}$. This technique has been used extensively to study membrane binding of the vesicular stomatitis virus M protein (2, 7, 8) and has also been

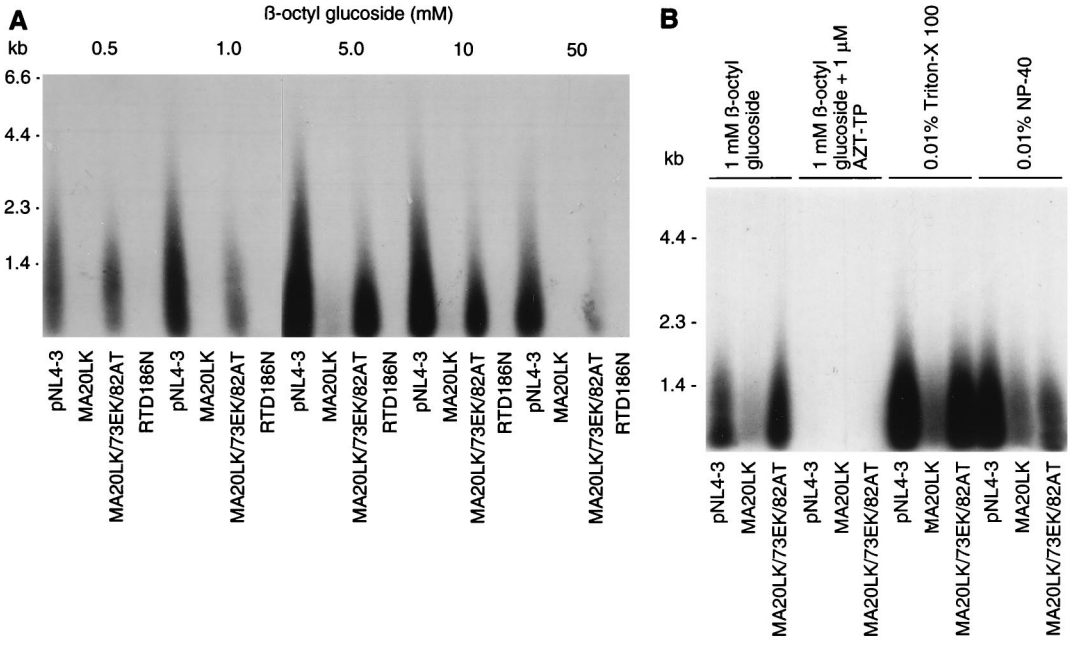

FIG. 5. ERT activities of wt, 20LK, and 20LK/73EK/82AT virions. (A) Virions normalized for exogenous RT activity were permeabilized with different concentrations of β-octyl glucoside. The RT active-site mutant RT/D186N (10) was included as a negative control. Similar results were obtained when virion normalization was based on p24 concentration. (B) Virions were permeabilized with either 1 mM β-octylglucoside, 0.01% Triton X-100, or 0.01% NP-40 as indicated. A set of samples was treated with 1 μM zidovudine triphosphate (AZT-TP) as an additional negative control.

applied to the analysis of HIV-1 Gag membrane binding (38, 47). To eliminate differences in Gag expression resulting from differential rates of PR-mediated Gag processing observed with residue 20 mutants (30) HeLa cells were transfected with PR^- derivatives of pNL4-3 (26) containing wt or mutant MA coding regions. Two days posttransfection, postnuclear supernatants were prepared and subjected to membrane flotation analysis as described in Materials and Methods. In these assays, membrane floats from the bottom of the centrifuge tube to the interface between the 10 and 65% sucrose layers upon centrifugation. Thus, the extent of membrane binding is indicated by comparing the amount of material at the 10-to-65% interface (fractions 3 and 4) to the amount remaining in the bottom fractions (fractions 9 and 10). As controls, we analyzed the distribution of two membrane proteins: the HIV-1 transmembrane Env glycoprotein gp41, and the endoplasmic reticulum-resident protein calnexin. Both proteins were found almost exclusively in fractions 3 and 4 following ultracentrifugation (Fig. 6; data not shown), confirming the presence of the majority of cellular membranes in these fractions. For wt $Pr55^{Gag}$, approximately 40% of Gag is detected in membrane-containing fractions 3 and 4, (Fig. 6A), in agreement with our previous findings (38). As expected, a myristylation-defective Gag mutant showed a significant defect in membrane binding, with 0.8 to 3% of $Pr55^{Gag}$ found in fractions 3 and 4 (38; data not shown). In the case of 20LK, the percentage of $Pr55^{Gag}$ in the membrane-containing fractions is significantly increased relative to that of the wt (on average, approximately 75% of $Pr55^{Gag}$ is present in fractions 3 and 4), confirming that the 20LK mutation increases Gag membrane binding (30, 38). Intriguingly, the 20LK/73EK/82AT mutant binds membrane as efficiently as does 20LK (Fig. 6A), with approximately 75% of $Pr55^{Gag}$ observed in fractions 3 and 4. Thus, the 20LK-induced increase in $Pr55^{Gag}$ membrane binding is not reversed by the 73EK/82AT changes. Consistent with these membrane flotation results, we also observed in cell fractionation assays that the pronounced 20LK-induced increase in the amount of Gag recovered in the pellet fraction after high-speed ultracentrifugation (30) was not reversed by the 20LK/73EK/82AT mutations (data not shown).

Since the NC domain of Gag has been reported to influence the binding of HIV-1 Gag to membrane, perhaps due to its role in promoting Gag multimerization (40, 44), we also analyzed membrane binding in the context of a truncated Gag [which we refer to as p41 (MA-CA)] containing only MA and CA (38; see Materials and Methods). Consistent with the results obtained with full-length $Pr55^{Gag}$, the 20LK and 20LK/73EK/82AT p41 (MA-CA) mutants show significant increases in membrane binding relative to the wt (Fig. 6B); the fraction of Gag present in fractions 3 and 4 was increased, relative to that of the wt, by approximately 1.7-fold for both 20LK and 20LK/73EK/82AT.

During or shortly after virus release from the infected cell, the viral PR cleaves $Pr55^{Gag}$ to the mature Gag proteins MA, CA, NC, and p6. The data presented in Fig. 6A and B indicate that the revertant changes do not affect the membrane-binding properties of the 20LK mutant in the context of $Pr55^{Gag}$ or the truncated p41 (MA-CA) Gag. However, since the 20LK mutant is defective at a step in the virus life cycle when the mature Gag products predominate, we felt it was important to assess the effect of the 20LK and 20LK/73EK/82AT mutations on membrane binding in the context of the mature MA protein. Accordingly, we introduced the mutations into a pNL4-3 derivative in which a stop codon was present immediately after the p17 (MA) coding region (38; see Materials and Methods). We then compared the wt, 20LK, and 20LK/73EK/82AT MA proteins for membrane binding by membrane flotation centrifugation. Approximately 12% of wt p17 (MA) was observed in the membrane-containing fractions, whereas both the 20LK and 20LK/73EK/82AT mutants showed 50 to 55% of p17

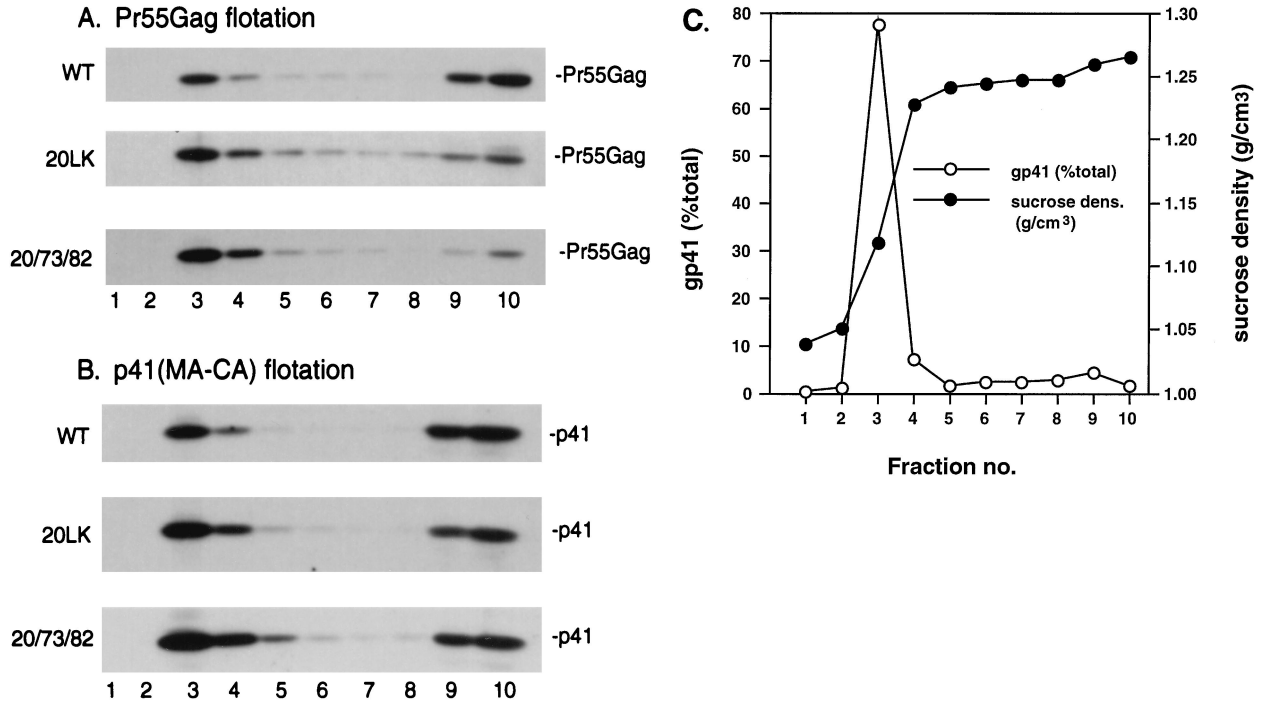

FIG. 6. Effects of MA mutations on Gag membrane binding analyzed by membrane flotation centrifugation. HeLa cells were transfected with a pNL4-3/PR$^-$ (A) or pNL4-3/p41stop (B) molecular clone or derivatives containing the 20LK or 20LK/73EK/82AT mutations (Materials and Methods). The pNL4-3/PR$^-$ clone expresses full-length Pr55^{Gag}, and pNL4-3/p41stop expresses a truncated Gag [p41 (MA-CA)] composed of MA and CA (see Materials and Methods). Postnuclear supernatants were prepared and subjected to membrane flotation centrifugation as described in Materials and Methods, during which membrane-bound material floats to the interface between 10 and 65% sucrose (fractions 3 and 4). Ten fractions were removed from the tops of the gradients and analyzed by SDS-PAGE followed by Western blotting with AIDS patient serum. Blots were reprobed with anti-gp41 antibody (C); and the amount of gp41 in each fraction (determined by densitometry scanning) was plotted against the concentration of sucrose in each fraction (measured with a refractometer).

(MA) in fractions 3 and 4. Thus, 20LK/73EK/82AT does not reverse the 20LK-imposed increase in membrane binding in the context of Pr55^{Gag}, p41 (MA-CA), or p17 (MA).

Analysis of virion density and composition: effects of detergent treatment. The results obtained by PCR, ERT, and single-cycle infectivity assays strongly suggested that 20LK/73EK/82AT had repaired defects in these assays imposed by mutation at residue 20, allowing the revertant virus to replicate with near-wt kinetics. To explore further the biochemical properties of the revertant virus, we compared the densities of wt, 20LK, and 20LK/73EK/82AT mutant virions. HeLa cells, transfected with wt or mutant molecular clones, were metabolically labeled with [^{35}S]Cys. Virions were pelleted from the labeled HeLa cell supernatant, resuspended, and loaded onto 20-to-70% sucrose gradients. Fractions were removed from the gradients and analyzed by RT assay. Twelve fractions (1 to 12) were collected, and the material at the bottom of the ultracentrifuge tube (the pellet fraction [P]) was resuspended and analyzed also. In parallel, material from each fraction was directly subjected to SDS-PAGE; labeled viral proteins were visualized by fluorography (shown for the wt in Fig. 7A). Direct visualization of virion proteins without immunoprecipitation avoids problems arising from differential antiserum reactivity to Gag mutants. The majority of virion proteins sedimented to fractions 4 to 6, at a density reported for virions (1.14 to 1.18 g/ml). Some material was also observed near the top or bottom of the gradients. The pattern of protein distribution (shown for the wt in Fig. 7A) indicated no differences in the density or composition of wt, 20LK, or 20LK/73EK/82AT virions (data not shown). In separate experiments, electron microscopy was performed on wt, 20LK, and 20LK/73EK/82AT virions; no morphological differences between the wt and mutant virions were observed (data not shown).

We next assessed the impact of detergent treatment on wt, 20LK, or 20LK/73EK/82AT virions. Labeled virions, prepared by ultracentrifugation as described above, were treated with 0.15% NP-40 for 15 min, and the resulting material was run over 20-to-70% sucrose gradients. Fractions were removed from the gradients and analyzed directly by SDS-PAGE and fluorography (Fig. 7B; see Materials and Methods). Following detergent treatment, three peaks of viral proteins were readily observed: one peak, located near the tops of the gradients (fractions 1 to 4), was comprised of free, detergent-solubilized proteins. The second peak was located in fraction 9. The density of this fraction (1.24 to 1.29 g/ml) is consistent with that of retroviral cores (27, 33, 50). The third peak, found at the bottom of the ultracentrifuge tubes, represented aggregated viral proteins. The wt and 20LK detergent-treated protein profiles appeared to be quite similar. The vast majority of MA (and gp120 [data not shown]) was present in the free protein fractions at the top of the gradient, while a substantial amount of CA and integrase was present in the dense peaks in fractions 9 and 11 to 12. Intriguingly, 20LK/73EK/82AT gradients showed a very different pattern: we observed a marked increase in the amount of p17 (MA) present in the core-like fraction (fraction 9) and in the bottom fractions (11, 12, and P). The amount of MA observed in the top fractions of 20LK/73EK/82AT gradients was correspondingly reduced. These results were highly reproducible in a number of experiments and were also observed in 10-to-60% and 20-to-60% sucrose gradients (data not shown) and under different detergent conditions (see Materials and Methods). The identities of the indi-

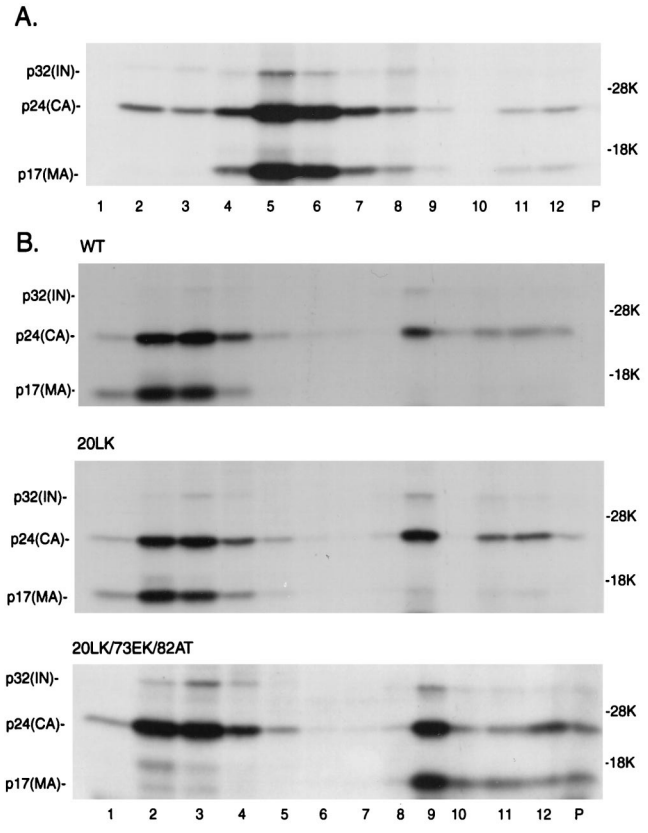

FIG. 7. Sucrose gradient analysis of wt and mutant virions before (A) and after (B) detergent treatment. HeLa cells were transfected with the wt or mutant pNL4-3 molecular clones and metabolically labeled with [^{35}S]Cys; supernatants were harvested, and virions were pelleted in an ultracentrifuge. In panel A, pelleted wt NL4-3 virions were loaded onto a 20-to-70% sucrose gradient; twelve fractions (1 to 12) and a pellet fraction (P) were removed from the tops of the gradients following ultracentrifugation and analyzed directly by SDS-PAGE. In panel B, pelleted wt and mutant virions were treated for 15 min with NP-40 at a 0.075% final concentration before ultracentrifugation and SDS-PAGE analysis as described in Materials and Methods. The values on the right are molecular sizes in kilodaltons.

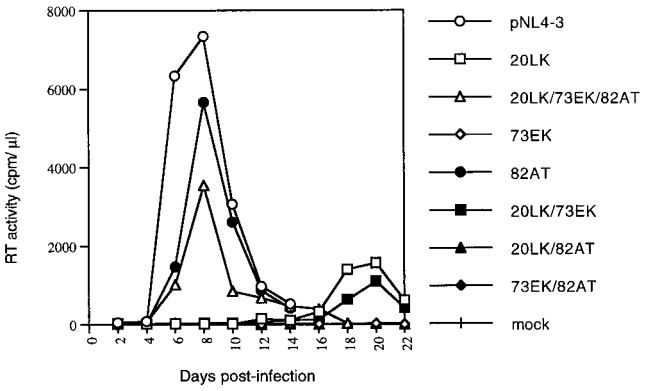

FIG. 8. Virus replication kinetics of 20LK revertant-derived MA mutants. HeLa cells were transfected with the indicated molecular clones. Virus stocks were harvested, normalized for RT activity, and used to infect H9 cells. Cells were split 1:3 every 2 days; the RT activities in culture supernatants were determined for each time point.

cated proteins were confirmed by immunoprecipitation with HIV-1-specific antiserum; the 18-kDa band detected above p17 (MA) appeared to be nonviral in origin, as it was not immunoprecipitated with HIV-1-specific antiserum (data not shown).

Analysis of single and double mutants. Since the 20LK/73EK/82AT revertant virus contains two second-site changes in addition to the original 20LK mutation, we sought to determine whether both changes were necessary to confer the reverted phenotype. To this end, we constructed 20LK/73EK and 20LK/82AT double mutants and determined their replication kinetics in H9 cells (Fig. 8). 20LK/73EK displayed a marked (12-day) delay in replication relative to the wt, while 20LK/82AT failed to replicate. Thus, in the context of the original mutation at residue 20, only 20LK/73EK/82AT showed a reverted phenotype, indicating that both second-site changes are necessary to confer reversion. We also constructed 73EK and 82AT single mutants to assess the effects of these second-site changes in the context of the wt molecular clone. The 82AT single mutant grew with essentially wt kinetics, whereas 73EK demonstrated either no RT production in infected cultures (Fig. 8) or a marked delay in replication kinetics (data not shown). The 73EK/82AT double mutant failed to replicate.

To investigate the effects of these single and double mutants on Gag processing and virus assembly and release, cell- and virion-associated proteins produced from transfected HeLa cells were analyzed by immunoprecipitation analysis (Fig. 9). As discussed above, mutation at residue 20 leads to an increase in Pr55^{Gag} processing (30) which is not reversed by the 73EK/82AT changes. All 20LK-containing mutants also showed a low level of cell-associated Pr55^{Gag} (Fig. 9A), resulting in part from a reduced immunoreactivity of mutant Pr55^{Gag} with the antiserum used in the immunoprecipitations (30). The 20LK/82AT double mutant displayed a marked virus assembly and release defect (Fig. 9A). Analysis of mutants containing single and double amino acid substitutions indicated that 82AT caused a modest reduction in the release of virion-associated p24 (CA) (50% of that of the wt) and a slight defect in Env incorporation. Both 73EK and 73EK/82AT showed a striking defect in virus release, as evidenced by the approximately 10-fold reduction in the release of virion-associated p24 (Fig. 9B).

DISCUSSION

In this study, we identified and characterized a viral revertant of the 20LK HIV-1 MA mutant. The revertant acquired second-site changes at MA residues 73 (73EK) and 82 (82AT) while retaining the 20LK substitution. Analysis of virus replication kinetics, single-cycle infectivity assays, and PCR amplification of viral DNA postinfection all indicated that the 20LK/73EK/82AT triple mutant largely reversed the defect evident with 20LK in these assays. In addition, the ERT defect evident with the original 20LK mutant was repaired in the revertant virus. Interestingly, however, the increased Gag membrane binding observed with 20LK was maintained in the revertant. Detergent treatment of wt and mutant virions, followed by sucrose gradient ultracentrifugation, revealed that detergent-resistant complexes prepared from wt and 20LK virions lacked or contained only a small amount of MA, whereas this protein was abundantly present in 20LK/73EK/82AT complexes.

It is unclear by what mechanism the 73EK and 82AT changes reverse the biological defect imposed by the 20LK substitution. Both residues 73 and 82 are in MA helix 4 (Fig. 10); although much of this helix is buried in the three-dimensional structure of MA, residue 73 is located at the putative trimer interface (24). The residue 73 and 82 changes could therefore influence the overall structure of MA or influence the formation of trimeric or other higher-order MA com-

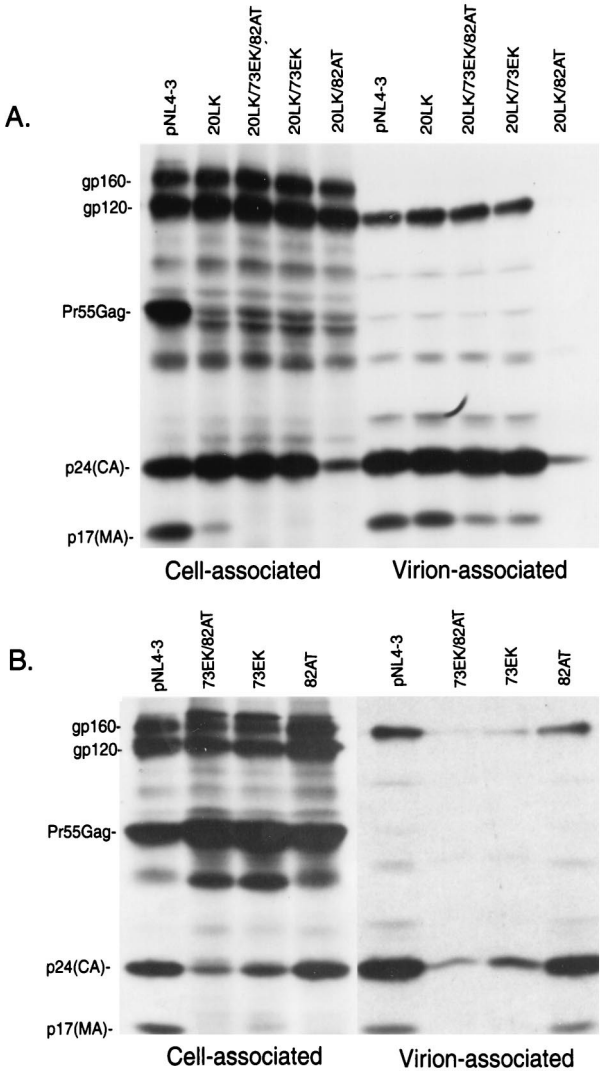

FIG. 9. Immunoprecipitation analysis of MA mutants. HeLa cells were transfected with the indicated molecular clones. One day posttransfection, cells were metabolically labeled overnight with [^{35}S]Cys. Virions from the labeled cell supernatant were pelleted in an ultracentrifuge. Cell and virion lysates were prepared and immunoprecipitated with AIDS patient serum as described in Materials and Methods. The positions of Env glycoprotein precursor gp160, mature surface Env glycoprotein gp120, Gag precursor Pr55^{Gag}, and the mature p24 (CA) and p17 (MA) proteins are indicated.

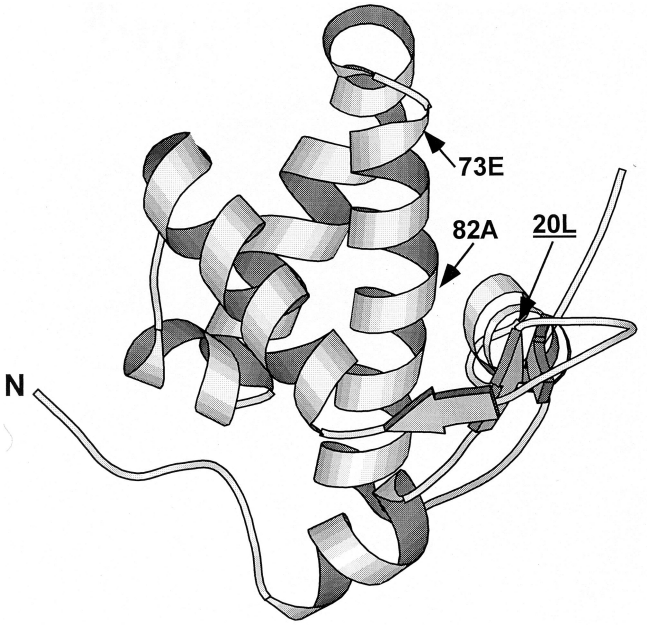

FIG. 10. Position of residues 20, 73, and 82 in the MA structure. Residue 20 is underlined; the N terminus of MA is indicated by the letter N. The structure was drawn by using the nuclear magnetic resonance data (MA residues 1 to 113) of Massiah et al. (34) with the MOLSCRIPT program (31). Since the indicated structure is truncated at MA residue 113, the long tail, which is predicted to project away from the membrane (24), is not shown.

plexes. This hypothesis is supported by our observation that the 73EK, 73EK/82AT, and 20LK/82AT mutations cause severe defects in virus particle production (Fig. 9). An assembly-release defect associated with the 73EK substitution is consistent with a previous report that described reduced virus production with a 69TE/73EK double mutant (5), and an association between trimer interface mutations and virus assembly defects has been reported (36).

Defects in ERT activity have been observed in studies involving several HIV-1 proteins distinct from RT itself. For example, truncations within the cytoplasmic domain of gp41 reduced the amount of endogenous reverse transcription in the absence of added detergent; it was postulated that the long cytoplasmic tail of gp41 rendered the viral envelope permeable to deoxyribonucleoside triphosphates (53). Virions produced in the absence of Tat displayed defects in reverse transcription both early postinfection and in endogenous reactions (23). Mutation of Vif was also reported to disrupt reverse transcription in endogenous assays (21). In our studies, we observed that MA residue 20 mutations induced ERT defects and that the magnitude of the defects correlated with the severity of the mutations in terms of virus replication and infectivity (30). In the current study, we observed that the 20LK revertant 20LK/73EK/82AT displayed markedly improved ERT activity relative to that of 20LK. Together, these results suggest that the ERT defect observed with the residue 20 mutations is biologically meaningful, although the mechanism by which the ERT defect is induced is unknown. Neither virion RT activity in exogenous assays nor the level of mature RT products in virions is affected by the residue 20 MA mutations (30). Although we did not examine the incorporation of the tRNA^{Lys} primer into virions, the fact that early reverse transcription products are initially synthesized at near-wt levels postinfection (Fig. 4) (30) suggests that initiation of reverse transcription is not defective. We hypothesize that the residue 20 mutations, particularly 20LK, affect some aspect of core structure or permeability such that virions are defective in ERT assays. It is noteworthy that MA residue 20 mutants resemble Vif-defective mutants in two respects: they can both induce ERT defects (21) and appear to cause a degradation of reverse transcription products early postinfection (45). In other respects, however, the Vif and MA mutants differ; in particular, MA residue 20 mutants show significant replication defects in all of the cell types and lines tested (30), whereas the effects of Vif mutation are markedly cell type dependent (19, 43).

Analysis of the protein profiles obtained by treating wt and mutant virions with detergent and running the resulting preparations through sucrose gradients revealed an unexpected finding: whereas the majority of wt and 20LK MA shifted to the top of the gradient upon detergent treatment, 20LK/73EK/82AT MA remained largely associated with high-density com-

plexes present at or near the bottom of the sucrose gradients. The 82AT mutant also showed this property, although to a somewhat lesser extent than 20LK/73EK/82AT (29). While we do not have definitive proof that the complexes observed in fraction 9 of 20-to-70% sucrose gradients (Fig. 7) are viral cores, their density and protein composition are consistent with cores or core-like complexes (27, 33, 50), and RNA dot blot analysis indicated that the wt, 20LK, and 20LK/73EK/82AT peak core-like fractions contained viral RNA (29). In any case, it is clear that the behavior of 20LK/73EK/82AT MA is markedly changed in these assays, suggesting an alteration in MA-MA or MA-core interactions. This observation is reminiscent of a previous finding of Reicin et al. (41), who observed an apparent detergent-resistant aggregation of MA caused by two small insertions in MA. In the latter study, however, the detergent-resistant material was not analyzed by sucrose gradient centrifugation.

It is intriguing to consider the possibility that the 20LK/73EK/82AT changes alter MA-MA or MA-core interactions in light of our recent finding that the 20LK/73EK/82AT mutant blocked PR-mediated cleavage of the murine leukemia virus (MuLV) transmembrane (TM) Env protein in HIV-1 virions pseudotyped with MuLV Env (28). We speculate that the 20LK/73EK/82AT mutations alter the organization of higher-order MA complexes such that accessibility of PR to the MuLV TM Env protein is obstructed. As is the case with MA distribution in sucrose gradients (29), the 82AT mutant shows an MuLV TM cleavage phenotype intermediate between the wt and 20LK/73EK/82AT (28). It will be of interest to compare the structures of the wt and 20LK/73EK/82AT mutant MA proteins by nuclear magnetic resonance methods and X-ray crystallography.

We have previously postulated that binding of Gag to membrane must be balanced to ensure proper Gag function during early and late stages of the virus life cycle (30, 38). Decreased Gag membrane binding caused by mutations near the N terminus of MA impairs virus assembly and release (38), whereas increased membrane binding observed with MA residue 20 mutations or an amino acid 97 substitution is associated with defects in early events postinfection (29, 30, 38). The correlation between increased membrane binding and an early defect in the virus life cycle could result from the retention of MA at the lipid bilayer after membrane fusion; if a population of MA molecules is associated with the viral core and/or preintegration complex (4, 20, 35), this retention at the membrane could cause an instability of the core or preintegration complex and the degradation of viral RNA and/or DNA during reverse transcription. This interpretation would rationalize the 20LK defect with the observation that under some conditions, the early events in HIV-1 replication can proceed in the absence of MA (42). It is interesting that the 20LK/73EK/82AT mutant has largely reversed the 20LK-imposed virus replication defect without affecting the increased Gag membrane binding induced by 20LK (Fig. 6). Perhaps altered MA-MA or MA-core interactions observed with 20LK/73EK/82AT mutant MA reverses the instability induced by increased membrane binding. Future studies will be aimed at further defining the function of MA in HIV-1 replication and elucidating the role that Gag membrane binding plays both early and late in the virus life cycle.

ACKNOWLEDGMENTS

We thank R. Willey and T. Murakami for critical review of the manuscript and J. Orenstein for performing electron microscopy. The following reagents were obtained through the NIH AIDS Research Reference and Reagent Program: HIV-1 patient immunoglobulin (from A. Prince) and HIV-1 neutralizing sera (from L. Vujcic).

R.E.K. was supported in part by an Australian Commonwealth AIDS Research Grant fellowship.

REFERENCES

1. **Adachi, A., H. E. Gendelman, S. Koenig, T. Folks, R. Willey, A. Rabson, and M. A. Martin.** 1986. Production of acquired immunodeficiency syndrome-associated retrovirus in human and nonhuman cells transfected with an infectious molecular clone. J. Virol. **59:**284–291.
2. **Bergmann, J. E., and P. J. Fusco.** 1988. The M protein of vesicular stomatitis virus associates specifically with the basolateral membranes of polarized epithelial cells independently of the G protein. J. Cell Biol. **107:**1707–1715.
3. **Bryant, M., and L. Ratner.** 1990. Myristoylation-dependent replication and assembly of human immunodeficiency virus 1. Proc. Natl. Acad. Sci. USA **87:**523–527.
4. **Bukrinsky, M. I., N. Sharova, T. L. McDonald, T. Pushkarskaya, W. G. Tarpley, and M. Stevenson.** 1993. Association of integrase, matrix, and reverse transcriptase antigens of human immunodeficiency virus type 1 with viral nucleic acids following acute infection. Proc. Natl. Acad. Sci. USA **90:**6125–6129.
5. **Cannon, P. M., S. Matthews, N. Clark, E. D. Byles, O. Iourin, D. J. Hockley, S. M. Kingsman, and A. J. Kingsman.** 1997. Structure-function studies of the human immunodeficiency virus type 1 matrix protein, p17. J. Virol. **71:**3474–3483.
6. **Casella, C. R., L. J. Raffini, and A. T. Panganiban.** 1997. Pleiotropic mutations in the HIV-1 matrix protein that affect diverse steps in replication. Virology **228:**294–306.
7. **Chong, L. D., and J. K. Rose.** 1994. Interactions of normal and mutant vesicular stomatitis virus matrix proteins with the plasma membrane and nucleocapsids. J. Virol. **68:**441–447.
8. **Chong, L. D., and J. K. Rose.** 1993. Membrane association of functional vesicular stomatitis virus matrix protein in vivo. J. Virol. **67:**407–414.
9. **Dorfman, T., F. Mammano, W. A. Haseltine, and H. G. Gottlinger.** 1994. Role of the matrix protein in the virion association of the human immunodeficiency virus type 1 envelope glycoprotein. J. Virol. **68:**1689–1696.
10. **Engelman, A., G. Englund, J. M. Orenstein, M. A. Martin, and R. Craigie.** 1995. Multiple effects of mutations in human immunodeficiency virus type 1 integrase on viral replication. J. Virol. **69:**2729–2736.
11. **Folks, T., S. Benn, A. Rabson, T. Theodore, M. D. Hoggan, M. Martin, M. Lightfoote, and K. Sell.** 1985. Characterization of a continuous T-cell line susceptible to the cytopathic effects of the acquired immunodeficiency syndrome (AIDS)-associated retrovirus. Proc. Natl. Acad. Sci. USA **82:**4539–4543.
12. **Freed, E. O.** 1998. HIV-1 Gag proteins: diverse functions in the virus life cycle. Virology **251:**1–15.
13. **Freed, E. O., E. L. Delwart, G. L. Buchschacher, Jr., and A. T. Panganiban.** 1992. A mutation in the human immunodeficiency virus type 1 transmembrane glycoprotein gp41 dominantly interferes with fusion and infectivity. Proc. Natl. Acad. Sci. USA **89:**70–74.
14. **Freed, E. O., and M. A. Martin.** 1996. Domains of the human immunodeficiency virus type 1 matrix and gp41 cytoplasmic tail required for envelope incorporation into virions. J. Virol. **70:**341–351.
15. **Freed, E. O., and M. A. Martin.** 1994. Evidence for a functional interaction between the V1/V2 and C4 domains of human immunodeficiency virus type 1 envelope glycoprotein gp120. J. Virol. **68:**2503–2512.
16. **Freed, E. O., and M. A. Martin.** 1995. Virion incorporation of envelope glycoproteins with long but not short cytoplasmic tails is blocked by specific, single amino acid substitutions in the human immunodeficiency virus type 1 matrix. J. Virol. **69:**1984–1989.
17. **Freed, E. O., D. J. Myers, and R. Risser.** 1989. Mutational analysis of the cleavage sequence of the human immunodeficiency virus type 1 envelope glycoprotein precursor gp160. J. Virol. **63:**4670–4675.
18. **Freed, E. O., J. M. Orenstein, A. J. Buckler-White, and M. A. Martin.** 1994. Single amino acid changes in the human immunodeficiency virus type 1 matrix protein block virus particle production. J. Virol. **68:**5311–5320.
19. **Gabuzda, D. H., K. Lawrence, E. Langhoff, E. Terwilliger, T. Dorfman, W. A. Haseltine, and J. Sodroski.** 1992. Role of *vif* in replication of human immunodeficiency virus type 1 in $CD4^+$ T lymphocytes. J. Virol. **66:**6489–6495.
20. **Gallay, P., S. Swingler, J. Song, F. Bushman, and D. Trono.** 1995. HIV nuclear import is governed by the phosphotyrosine-mediated binding of matrix to the core domain of integrase. Cell **83:**569–576.
21. **Goncalves, J., Y. Korin, J. Zack, and D. Gabuzda.** 1996. Role of Vif in human immunodeficiency virus type 1 reverse transcription. J. Virol. **70:**8701–8709.
22. **Gottlinger, H. G., J. G. Sodroski, and W. A. Haseltine.** 1989. Role of capsid precursor processing and myristoylation in morphogenesis and infectivity of human immunodeficiency virus type 1. Proc. Natl. Acad. Sci. USA **86:**5781–5785.
23. **Harrich, D., C. Ulich, L. F. Garcia-Martinez, and R. B. Gaynor.** 1997. Tat is required for efficient HIV-1 reverse transcription. EMBO J. **16:**1224–1235.
24. **Hill, C. P., D. Worthylake, D. P. Bancroft, A. M. Christensen, and W. I.**

Sundquist. 1996. Crystal structures of the trimeric human immunodeficiency virus type 1 matrix protein: implications for membrane association and assembly. Proc. Natl. Acad. Sci. USA **93:**3099–3104.
25. **Hirt, B.** 1967. Selective extraction of polyoma DNA from infected mouse cell cultures. J. Mol. Biol. **26:**365–369.
26. **Huang, M., J. M. Orenstein, M. A. Martin, and E. O. Freed.** 1995. $p6^{Gag}$ is required for particle production from full-length human immunodeficiency virus type 1 molecular clones expressing protease. J. Virol. **69:**6810–6818.
27. **Kewalramani, V. N., and M. Emerman.** 1996. Vpx association with mature core structures of HIV-2. Virology **218:**159–168.
28. **Kiernan, R. E., and E. O. Freed.** 1998. Cleavage of the murine leukemia virus transmembrane env protein by human immunodeficiency virus type 1 protease: transdominant inhibition by matrix mutations. J. Virol. **72:**9621–9627.
29. **Kiernan, R. E., and E. O. Freed.** Unpublished results.
30. **Kiernan, R. E., A. Ono, G. Englund, and E. O. Freed.** 1998. Role of matrix in an early postentry step in the human immunodeficiency virus type 1 life cycle. J. Virol. **72:**4116–4126.
31. **Kraulis, P. J.** 1991. MOLSCRIPT: a program to produce both detailed and schematic plots of protein structure. J. Appl. Crystallogr. **24:**946–950.
32. **Lee, P. P., and M. L. Linial.** 1994. Efficient particle formation can occur if the matrix domain of human immunodeficiency virus type 1 Gag is substituted by a myristylation signal. J. Virol. **68:**6644–6654.
33. **Liu, H., X. Wu, M. Newman, G. M. Shaw, B. H. Hahn, and J. C. Kappes.** 1995. The Vif protein of human and simian immunodeficiency viruses is packaged into virions and associates with viral core structures. J. Virol. **69:**7630–7638.
34. **Massiah, M. A., M. R. Starich, C. Paschall, M. F. Summers, A. M. Christensen, and W. I. Sundquist.** 1994. Three-dimensional structure of the human immunodeficiency virus type 1 matrix protein. J. Mol. Biol. **244:**198–223.
35. **Miller, M. D., C. M. Farnet, and F. D. Bushman.** 1997. Human immunodeficiency virus type 1 preintegration complexes: studies of organization and composition. J. Virol. **71:**5382–5390.
36. **Morikawa, Y., W. H. Zhang, D. J. Hockley, M. V. Nermut, and I. M. Jones.** 1998. Detection of a trimeric human immunodeficiency virus type 1 Gag intermediate is dependent on sequences in the matrix protein, p17. J. Virol. **72:**7659–7663.
37. **Myers, G., B. H. Hahn, J. W. Mellors, L. E. Henderson, B. Korber, K.-T. Jeang, F. E. McCutchan, and G. N. Pavlakis.** 1995. Human retroviruses and AIDS. A compilation and analysis of nucleic acid and amino acid sequences. Los Alamos National Laboratory, Los Alamos, N.Mex.
38. **Ono, A., and E. O. Freed.** 1999. Binding of human immunodeficiency virus type 1 Gag to membrane: role of the matrix amino terminus. J. Virol. **73:**4136–4144.
39. **Ono, A., M. Huang, and E. O. Freed.** 1997. Characterization of human immunodeficiency virus type 1 matrix revertants: effects on virus assembly, Gag processing, and Env incorporation into virions. J. Virol. **71:**4409–4418.
40. **Platt, E. J., and O. K. Haffar.** 1994. Characterization of human immunodeficiency virus type 1 Pr55gag membrane association in a cell-free system: requirement for a C-terminal domain. Proc. Natl. Acad. Sci. USA **91:**4594–4598.
41. **Reicin, A. S., A. Ohagen, L. Yin, S. Hoglund, and S. P. Goff.** 1996. The role of Gag in human immunodeficiency virus type 1 virion morphogenesis and early steps of the viral life cycle. J. Virol. **70:**8645–8652.
42. **Reil, H., A. A. Bukovsky, H. R. Gelderblom, and H. G. Gottlinger.** 1998. Efficient HIV-1 replication can occur in the absence of the viral matrix protein. EMBO J. **17:**2699–2708.
43. **Sakai, H., R. Shibata, J. Sakuragi, S. Sakuragi, M. Kawamura, and A. Adachi.** 1993. Cell-dependent requirement of human immunodeficiency virus type 1 Vif protein for maturation of virus particles. J. Virol. **67:**1663–1666.
44. **Sandefur, S., V. Varthakavi, and P. Spearman.** 1998. The I domain is required for efficient plasma membrane binding of human immunodeficiency virus type 1 $Pr55^{Gag}$. J. Virol. **72:**2723–2732.
45. **Simon, J. H., and M. H. Malim.** 1996. The human immunodeficiency virus type 1 Vif protein modulates the postpenetration stability of viral nucleoprotein complexes. J. Virol. **70:**5297–5305.
46. **Sodroski, J., W. C. Goh, C. Rosen, K. Campbell, and W. A. Haseltine.** 1986. Role of the HTLV-III/LAV envelope in syncytium formation and cytopathicity. Nature **322:**470–474.
47. **Spearman, P., R. Horton, L. Ratner, and I. Kuli-Zade.** 1997. Membrane binding of human immunodeficiency virus type 1 matrix protein in vivo supports a conformational myristyl switch mechanism. J. Virol. **71:**6582–6592.
48. **Wang, C. T., Y. Zhang, J. McDermott, and E. Barklis.** 1993. Conditional infectivity of a human immunodeficiency virus matrix domain deletion mutant. J. Virol. **67:**7067–7076.
49. **Willey, R. L., J. S. Bonifacino, B. J. Potts, M. A. Martin, and R. D. Klausner.** 1988. Biosynthesis, cleavage, and degradation of the human immunodeficiency virus 1 envelope glycoprotein gp160. Proc. Natl. Acad. Sci. USA **85:**9580–9584.
50. **Yu, X., Z. Matsuda, Q. C. Yu, T. H. Lee, and M. Essex.** 1993. Vpx of simian immunodeficiency virus is localized primarily outside the virus core in mature virions. J. Virol. **67:**4386–4390.
51. **Yu, X., Q. C. Yu, T. H. Lee, and M. Essex.** 1992. The C terminus of human immunodeficiency virus type 1 matrix protein is involved in early steps of the virus life cycle. J. Virol. **66:**5667–5670.
52. **Yu, X., X. Yuan, Z. Matsuda, T. H. Lee, and M. Essex.** 1992. The matrix protein of human immunodeficiency virus type 1 is required for incorporation of viral envelope protein into mature virions. J. Virol. **66:**4966–4971.
53. **Zhang, H., G. Dornadula, P. Alur, M. A. Laughlin, and R. J. Pomerantz.** 1996. Amphipathic domains in the C terminus of the transmembrane protein (gp41) permeabilize HIV-1 virions: a molecular mechanism underlying natural endogenous reverse transcription. Proc. Natl. Acad. Sci. USA **93:**12519–12524.